13th World Conference on Earthquake Engineering
Vancouver, B.C., Canada
August 1-6, 2004
Paper No. 2481

APPLICATION OF CONTROL THEORY FOR OPTIMAL DESIGN OF ADDED VISCOUS AND FRICTION DAMPERS

David J. DOWDELL[1] and Carlos E. VENTURA[2]

SUMMARY

A general procedure has been developed for the optimal design of viscous and friction/hysteretic damper systems that can be applied to a broad range of practical structures subjected to earthquakes. The LQ control problem is first solved to establish a set of full state feedback gains that provide an optimal control of the structure, corresponding to an optimal balance between structural response and control effort. Varying the balance between structural response and control effort provides a method of adjusting the strength until the performance criteria are satisfied. A set of passive viscous dampers is proportioned based on matching the derived active control at the peak cycle determined using response spectral analysis. The amount of energy dissipated in the peak cycle of each damper is subsequently used to determine the friction slip forces or hysteretic yield forces corresponding to these viscous dampers. The theoretical basis for the proposed procedure is derived and illustrated using two examples - a uniform 4-story moment frame structure and an 18 DOF asymmetrical building. The 18DOF asymmetrical building example illustrates that the mathematical procedure can be implemented using any number of dampers.

INTRODUCTION

Structures subjected to seismic loads often benefit from increased damping to improve their performance. However, in the case of friction dampers, it has been shown that the distribution of slip loads is an important consideration in optimizing the performance of the structure [1]. Often to design passive, non-linear control systems in a structure, designers need to resort to trial and error time history analyses. As structures become more complex and irregular, this task becomes more onerous. Based on a methodology originally proposed by Reinhorn *et al.* [2] the authors have developed a procedure whereby viscous and friction dampers can be proportioned in a general structural system based on the principles and formulation of optimal control theory [3, 4]. Re-formulating the problem in state-space form and utilising the gain matrix associated with the LQ control as a basis, a procedure was devised for estimating passive viscous damping coefficients that closely match the performance of the active system. But rather than utilising a time history as a basis as in [2], a response spectrum analysis (RSA) procedure was developed to estimate the necessary response quantities. An RSA technique is preferable during initial design stages due to the rapid computation speed and direct computation of envelope values. It is expected that as more complex structures are considered, the advantages of computation speed will make this type of analysis preferable.

[1] Structural Engineer, BC Hydro Engineering, Burnaby, Canada. dave.dowdell@bchydro.com
[2] Professor, Civil Eng., University of British Columbia, Vancouver, Canada. ventura@civil.ubc.ca

The objective of this paper is to illustrate this proposed technique using two examples; a uniform 4-story shear structure and a more complex 18DOF asymmetrical building structure.

THEORETICAL BACKGROUND

Modern control theory is based on the state space formulation of the equation of motion for a structure. Please refer to Meirovitch [5] and Soong [6] for complete treatments of theory of structural control. The basic matrix equation of motion for a structure is given as

$$\dot{x} = Ax + Bu + Lg \tag{1}$$

in which x is a $2n$x1 state vector containing displacements and velocities for each degree of freedom. The $2n$x$2n$ matrix A, defined below, represents the structure's dynamics; the $2n$xm matrix B represents the locations of the m control forces contained in mx1 vector u; and the $2n$xk matrix L describes the influence of the k acceleration components in vector g, has on the masses of the structure. Equation 1 is a first order system of differential equations that represents the usual second order differential equation of motion. Substituting

$$x = \begin{bmatrix} \bar{x} \\ \dot{\bar{x}} \end{bmatrix};\ A = \begin{bmatrix} 0 & I \\ -M^{-1}K & -M^{-1}\tilde{C} \end{bmatrix};\ B = \begin{bmatrix} 0 \\ \bar{B} \end{bmatrix};\ L = \begin{bmatrix} 0 \\ \bar{L} \end{bmatrix} \tag{2}$$

where M, $\tilde{C}$ and K are the usual mass, damping and stiffness matrices, and $\bar{B}$ and $\bar{L}$ are chosen to represent the locations of the damper connection points and the locations of the excitation input, Equation 1 yields the usual second order equation of motion

$$M\ddot{\bar{x}} + \tilde{C}\dot{\bar{x}} + K\bar{x} = M\bar{B}u + M\bar{L}g \tag{3}$$

Defining the control force, u, as that arising from a set of passive dampers

$$u = DCx \tag{4}$$

where C is an observer matrix that is defined such that the product $y=Cx$ computes the set of velocities corresponding to each damper in their selected locations. Ultimately the objective of the passive control problem is to determine the diagonal matrix D that provides the optimum control force vector $u=Dy$ satisfying the performance criteria

$$J = \int_{t_0}^{t_f} \left(x^T Q x + u^T R u \right) dt \tag{5}$$

where J is the performance index to be minimized. The input matrices Q and R are the means by which the designer influences the sense of the optimality. The matrix Q represents the weighting placed on the state variables, and R is a weighting placed on the control forces. In this study, Q is taken as having the mass and stiffness on the main diagonal is such a way to represent the total kinetic and potential energy. The matrix R is set proportional to the identity matrix as $R=R_{factor}I$. Lower values of R_{factor} produce stronger control. Choosing Q and R in this way reduces the design problem to the selection of the single variable R_{factor}. The use of the performance index in Equation 5 considers the system dynamics in the process of determining an optimal response. In this way the design process is greatly simplified.

Before considering the passive system we shall first consider the solution of the full state feedback problem $u = Gx$, where G is the full state gain matrix. The well-known solution to this problem is [4, 5]

$$G = -\tfrac{1}{2} R^{-1} B^T P \tag{6}$$

where *P* is known as the Ricatti matrix satisfying the stationary matrix Ricatti equation

$$\dot{P} = -2Q - PA - A^T P + \tfrac{1}{2} PBR^{-1} B^T P = 0. \tag{7}$$

Full state feedback is not practical due to the unnecessary inclusion of inputs not associated with activation of the dampers. As an intermediate step we can compute a square gain matrix, $\hat{D}$, termed the observer feedback gain matrix, that uses only on the observed values, *y*, associated with damper velocities in implementing an active control. Use of this matrix eliminates the need to reconstruct the full state vector. Since it is required that $u = Gx = \hat{D}Cx$, $\hat{D}$ needs to be isolated from the equation

$$\tfrac{1}{2} R^{-1} B^T P = \hat{D} C \tag{8}$$

But since *C* is not a square matrix, the solution for $\hat{D}$ can only proceed in the least-squares sense. Recognizing that for many practical damper arrangements, the matrix CC^T is square and invertible, post multiplying Equation 8 by $C^T \left(CC^T\right)^{-1}$ yields the equation

$$\hat{D} = \tfrac{1}{2} R^{-1} B^T P C^T \left(CC^T\right)^{-1} \tag{9}$$

The resulting direct feedback matrix $\hat{D}$, however, is generally fully populated and thus contains active feedback that cannot be reproduced by a set of passive viscous dampers. The active component is contained in the off-diagonal terms. One method of determining the passive component of $\hat{D}$ is by simple truncation of the above matrix to the non-negative elements contained on the main diagonal, expressed as

$$D_{trunc} = diag^{+}\left(\hat{D}\right) \tag{10}$$

where the "+" sign indicates that only non-negative values are retained. This truncation procedure produces a set of damping coefficients that is significantly weaker than the active control upon which it is based. (See [3] for a more detailed account.)

Reinhorn, *et al.* [2] suggested using a time history input to determine the set of damping coefficients whose corresponding control force provides a best fit to that of the fully active (target) control. Although this method was shown to provide a good agreement between the active and passive system, it is valid only for a particular time history. The alternative procedure suggested here is to establish estimates of the viscous damping coefficients by computing the maximum desired force in each of the dampers, considered to be actuators in the fully active system and compare these forces to the maximum velocities experienced by the dampers of the controlled structure. Thus a set of estimated passive damping coefficients

$$D = diag\left(\frac{u_{\max}}{y_{\max}}\right) \tag{11}$$

is established. While $u_{\max}$ and $y_{\max}$ can be extracted from a time history, the method suggested herein is to use response spectrum analysis to provide estimates of these quantities consistent with a design spectra.

PROPOSED RESPONSE SPECTRUM ANALYSIS METHOD

In design, a structure is often required to survive an earthquake input expressed in terms of a response spectrum. Analysis based on response spectral analysis (RSA) using the design spectrum offers some distinct advantages over time history analysis: (1) required envelope values are obtained directly,

eliminating the need for the post-processing of time history data from trials using multiple earthquakes; and (2) computational efficiency can be gained through using a reduced number of modes in analysis. The challenge in application of modal analysis techniques to a structure with discrete dampers is that the mode shapes and frequencies of the structure are no longer real valued. However, with some extra effort, complex mode shapes can be carried through a RSA analysis. It is useful to remain within the state-space formulation as sub-critical and super-critical damped modes can be handled within a uniform procedure.

There are several commonly used methods of combining the modes to yield estimates of envelope results. One of the simplest and the one used here is the Square Root of the Sum of the Squares (SRSS) method. Further discussion of modal combinations, although important, is beyond the scope of this investigation.

Based on the SRSS estimates

$$u_{\max} = \sqrt{\sum_i (Gx_i)^2}; \quad y_{\max} = \sqrt{\sum_i (Cx_i)^2} \tag{12}$$

the damping coefficients of the added dampers can be estimated by Equation 11. The index *i* represents the mode number and x_i represents the corresponding mode shape contribution including response spectral and modal participation factors. Evaluation of the quantities in Equations 12 above requires special treatment due to the fact that the 2-n modes arising from the analysis of a structure with discrete dampers are not, in general, real valued. Recognising that complex valued modes exist in complex conjugate pairs, they can be pre-combined such that the real-valued mode shapes and participation factors remain. Details are contained in [3]. The key equations are provided below:

$$x_{\max} \cong 2\sqrt{\sum_{j=1}^{m} \left(\max\left(S_j^C\right)x_j^C\right)^2 + \left(\max\left(S_j^S\right)x_j^S\right)^2} \tag{13}$$

$$y_{\max} \cong 2\sqrt{\sum_{j=1}^{m} \left(\max\left(S_j^C\right)Cx_j^C\right)^2 + \left(\max\left(S_j^S\right)Cx_j^S\right)^2} \tag{14}$$

$$u_{\max} \cong 2\sqrt{\sum_{j=1}^{m} \left(\max\left(S_j^C\right)Gx_j^C\right)^2 + \left(\max\left(S_j^S\right)Gx_j^S\right)^2} \tag{15}$$

where

$$\max\left(S_j^C\right) = \max\left(\left|\int_0^t e^{\varsigma_j(t-\tau)}\cos\left(\omega_j(t-\tau)\right)\ddot{x}_g(\tau)d\tau\right|\right) \tag{16a}$$

and

$$\max\left(S_j^S\right) = \max\left(\left|\int_0^t e^{\varsigma_j(t-\tau)}\sin\left(\omega_j(t-\tau)\right)\ddot{x}_g(\tau)d\tau\right|\right) \tag{16b}$$

$$x_j^C = U_j^{\mathrm{Re}}P_j^{\mathrm{Re}} - U_j^{\mathrm{Im}}P_j^{\mathrm{Im}} \tag{17a}$$

and

$$x_j^S = U_j^{\mathrm{Im}}P_j^{\mathrm{Re}} + U_j^{\mathrm{Re}}P_j^{\mathrm{Im}} \tag{17b}$$

where, given $P_j^{\mathrm{Re}} = V_j^{\mathrm{Re}^T} L$ and $P_j^{\mathrm{Im}} = V_j^{\mathrm{Im}^T} L$. Real and imaginary quantities in equations 16 and 17 are extracted from Λ_i, U_i and V_i and represent respectively the eigenvalue, and right and left eigenvector of mode *i*, broken down as follows:

$$\begin{aligned} U_j &= U_j^{\mathrm{Re}} + iU_j^{\mathrm{Im}}; \quad \overline{U}_j = U_j^{\mathrm{Re}} - iU_j^{\mathrm{Im}}; \\ V_j &= V_j^{\mathrm{Re}} + iV_j^{\mathrm{Im}}; \quad \overline{V}_j = V_j^{\mathrm{Re}} - iV_j^{\mathrm{Im}}; \\ \Lambda_j &= \varsigma_j^{\mathrm{Re}} + i\omega_j^{\mathrm{Im}}; \quad \overline{\Lambda}_j = \varsigma_j^{\mathrm{Re}} - i\omega_j^{\mathrm{Im}}. \end{aligned} \tag{18}$$

Proposed method for selecting viscous dampers

The proposed method is summarised in the following steps:

1 formulate the system dynamics by defining the *A*, *B* and *C* matrices
2 estimate a value for R_{factor} to regulate the strength of the control to a desired level
3 establish the target (active) control by solving the time independent Ricatti matrix, Equation 7 and then Equation 6 to establish the full state gains, and, if desired, the observer feedback Equation 9
4 using the controlled system $(A+BG)$ or $(A+B\hat{D}C)$ as a target, perform a modal analysis to establish eigenvalues Λ, and the right and left eigenvectors *U* and *V* (Equations 18) and scaled mode shapes from Equations 17a and 17b
5 look up or otherwise establish response spectrum values of Equations 16a and 16b
6 with the controlled modes defined in Step 3 and the spectrum values of Step 4, perform the SRSS modal combinations to establish envelope damper velocities, y_{max}, and full state control forces, u_{max}, using Equations 14 and 15 and mode shapes
7 compute the viscous damping coefficients using Equation 11
8 perform a modal combination using Equation 13 to evaluate the structural performance using the selected control and compare to the design requirements of the structure
9 if necessary estimate a more appropriate value for R_{factor} and repeat Steps 3 through 9 until the structure performs as required.

Following these steps, a recommended set of viscous damping coefficients at the selected locations that satisfying the performance requirements will be obtained. If the intent is to design a set of friction dampers, additional steps are required and these are covered in the next section.

EXTENSION TO FRICTION DAMPERS

Rather than using viscous dampers, if it is desired to utilize friction dampers to dissipate energy, slip loads of friction dampers that provide damping approximately equivalent to the viscous dampers can be estimated using the concept of equivalent peak-cycle energy dissipation. This is assumed to occur at the fundamental period of the first mode of the structure. Two cases are considered, the case where the friction damper is supported by a brace that is essentially rigid, and the second case where the friction damper is supported by a brace that contains some undesirable flexibility. In the latter case, the flexibility of the brace supporting the dampers was assumed to have either stiffness *K*, either explicitly defined or related to the horizontal stiffness of the structure itself, i.e. $K=\alpha k$.

Rigid Brace

The energy dissipated by the viscous dampers in one cycle is equal to the area enclosed by the elliptical hysteresis loop and is determined by the following expression

$$E_v = \pi u_{\max} d_{\max} \tag{19}$$

The energy dissipated in a friction damper with a perfectly rigid brace is given as

$$E_f = 4 s d_{\max} \tag{20}$$

where s represents the slip force characteristic of the friction damper. Equating Equations 19 and 20 above and solving for the slip load *s* gives the result

$$s = \frac{\pi}{4} u_{\max} . \tag{21}$$

Flexible Brace

In the case of a flexible brace, the hysteresis loop characteristic of the brace and damper together has the form as shown in Figure 1. The energy enclosed by this hysteresis loop is given as

$$E_f = 4 s \left(d_{\max} - \frac{s}{K} \right) \tag{22}$$

and equating the energy of Equation 22 to Equation 19 yields the result

$$s = K \left(\frac{d_{\max}}{2} - \sqrt{\left(\frac{d_{\max}}{2} \right)^2 - \frac{\pi}{4} \frac{u_{\max} d_{\max}}{K}} \right) \tag{23}$$

which only has a solution if

$$d_{\max} > \frac{\pi u_{\max}}{K} \tag{24}$$

or, otherwise stated, the brace stiffness must satisfy the following

$$K > \frac{\pi u_{\max}}{d_{\max}} . \tag{25}$$

It is emphasized that the quantity *K* expresses unwanted stiffness in the bracing system connecting the friction damper to the rest of the structure, and is not necessarily under the control of the designer. Equation 23 assumes that the lower valued root of the energy balance equation is preferable both for economy and to permit the devices to dissipate energy during events that are smaller than the design event. Figure 1 illustrates the variability of the slip force with increasing brace stiffness above the limit indicated by Equation 25.

In order to evaluate the associated friction dampers using the energy balance procedure, it is necessary to extract estimates of the peak displacement to which the dampers are subjected. Using a modal analysis procedure similar to that used to establish u_{max} and y_{max}, d_{max} can be calculated using

$$d_{\max} = \sqrt{\sum_i \left(C_d x_i \right)^2} \tag{26}$$

where C_d is an observer set to identify the displacements. Observers C and C_d are related as follows

$$C = \begin{bmatrix} 0 \\ \overline{C} \end{bmatrix}; \; C_d = \begin{bmatrix} \overline{C} \\ 0 \end{bmatrix} \tag{27}$$

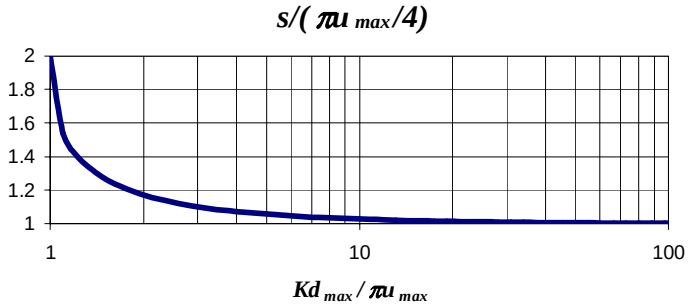

Figure 1. Friction slip force as a function of brace stiffness.

4DOF EXAMPLE

A uniform shear frame structure with friction dampers on each story is used as a simple example to illustrate application of the methods proposed and to compare with optimal friction dampers distributions evaluated previously. The structure and its key variables are defined in Figure 2 and the frequencies and damping ratios in each of the 4 modes are given in Table 1.

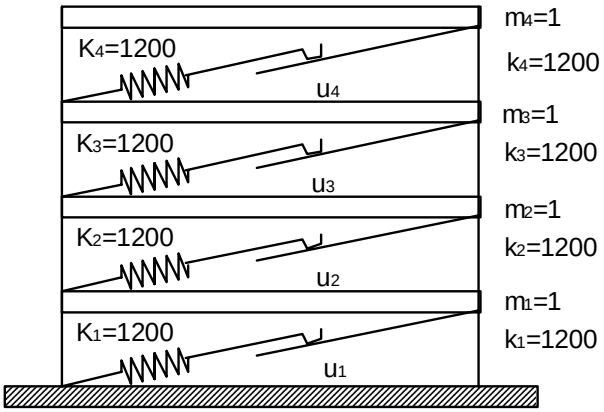

Figure 2. 4-Story friction damped structure.

Table 1. Uniform 4-story structure undamped response frequencies.

Mode	Circular Frequency (rad/sec)	Frequency (Hz)	Period (sec)	Damping (%)
1	12.0	1.92	0.552	2.5%
2	34.6	5.51	0.181	2.5%
3	53.1	8.45	0.118	3.3%
4	65.1	10.36	0.097	3.9%

The control corresponding to the choice of R=0.006I and R=0.00053I, are taken to represent a weak control and a strong control, respectively. Each are used to provide a comparison between the uncontrolled structure performance and the structural performance with (1) full state active controlled; (2) active direct (observer) feedback controlled; (3) passive viscous damped with damping coefficients chosen using the truncated observer matrix; and (4) passive viscous damped with damping coefficients chosen using the RSA technique to match the full state active feedback control response. Displacement and velocity envelopes obtained for each case under the input of the California 1940 Imperial Valley earthquake, El Centro N00E record as well as response time histories are compared in Figures 3 and 4. These plots indicate that, in general, the passive damped structure that was matched to the fully active

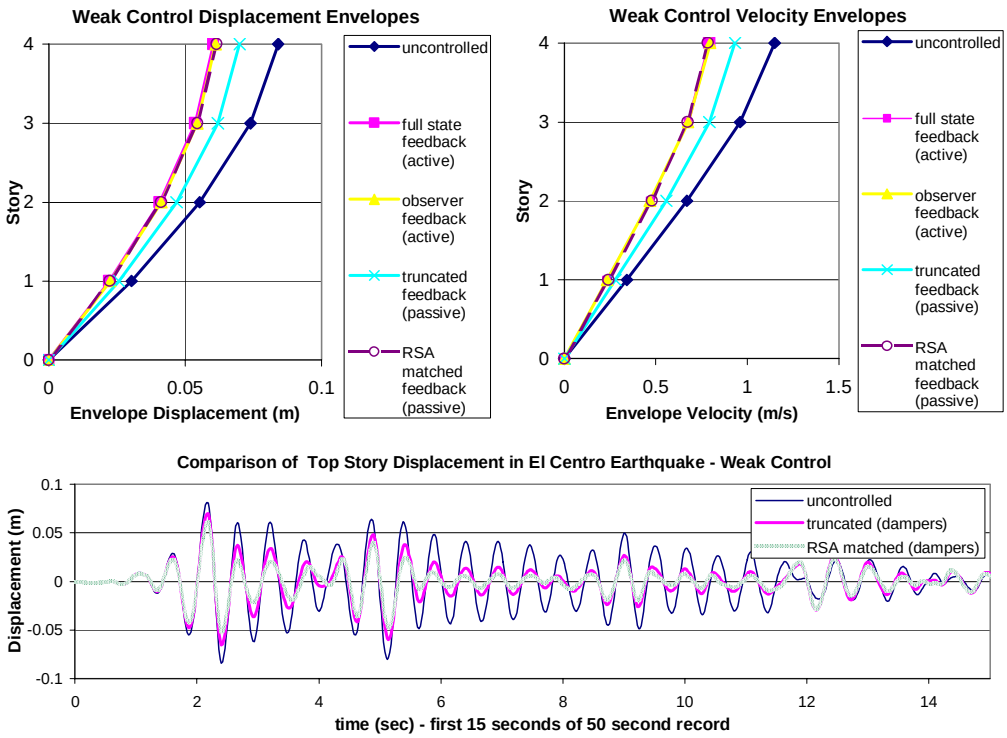

Figure 3. Comparison of uncontrolled, full-state, observer, truncated and RSA matched displacements and velocities of 4-story structure in El Centro earthquake record. Weak control -Rfactor=0.06

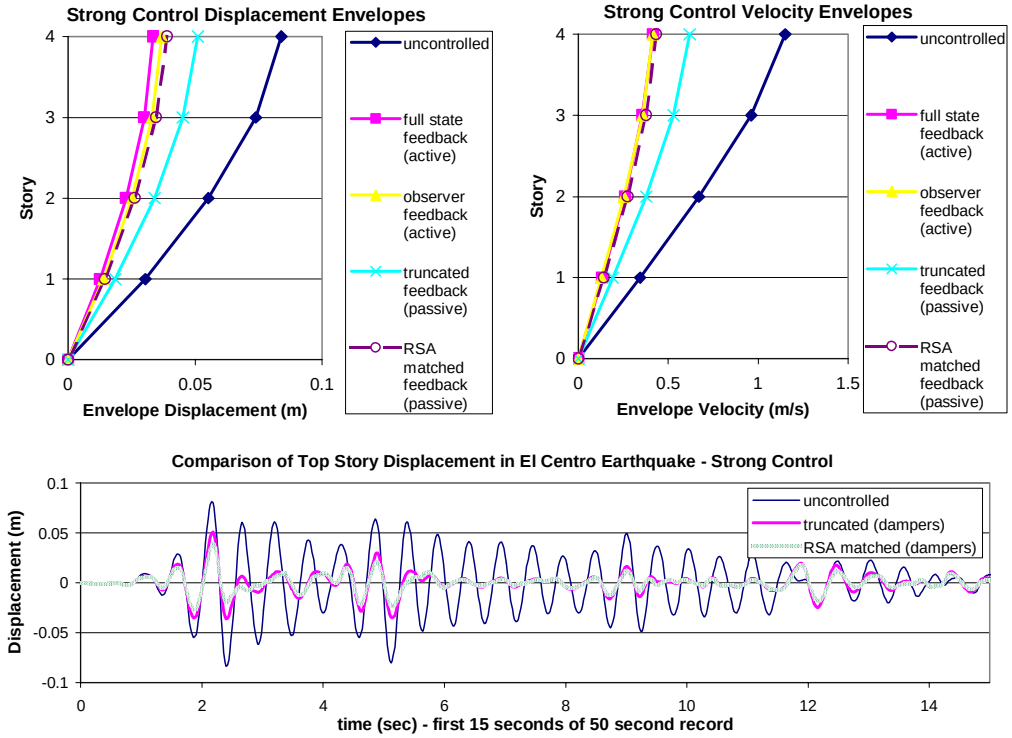

Figure 4. Comparison of uncontrolled, full-state, observer, truncated and RSA matched displacements and velocities of 4-story structure in El Centro earthquake record. Strong control - Rfactor=0.0053.

control (case 4) responded in a similar manner to the actively controlled structures (cases 1 and 2), while the dampers selected using the truncation method (case 3) produced a significantly weaker control, but still provided an improvement over the uncontrolled base case.

Next the control strength was varied over a range of possible values and the response quantities tracked. The viscous damping coefficients obtained using the matching technique as well as the corresponding slip loads evaluated using the peak-cycle energy dissipation relationships established for a flexible brace with the brace stiffness providing a horizontal stiffness chosen as twice the frame stiffness. Table 2 contains the obtained values for two events, the El Centro N00E record specified above, and the California 1971 San Fernando Earthquake Lake Hughes Array Station 12 record N21E. Spectral values for each analysis were established using Equations 16a and 16b prior to performing modal combinations by the SRSS method.

Table 2. Comparison of computed damping coefficients and slip loads

Earthquake	Run	Rfactor	Damping Coefficient* (kN.s/m)				Slip Load: K=2400 (α=2)				Drift Ratio Demands ** (3m storey height)			
			1	2	3	4	1	2	3	4	1	2	3	4
	1	0.060	15.8	14.2	12.3	11.1	2.96	2.75	2.25	1.30	**0.0074**	**0.0062**	0.0043	0.0022
	2	0.040	19.9	17.8	15.5	14.0	3.47	3.24	2.65	1.53	**0.0069**	**0.0058**	0.0040	0.0021
	3	0.027	24.8	22.4	19.4	17.6	4.02	3.77	3.08	1.78	**0.0064**	**0.0053**	0.0037	0.0019
	4	0.0178	29.3	28.0	24.3	22.0	4.61	4.33	3.54	2.05	**0.0059**	0.0048	0.0034	0.0018
El Centro	5	0.0119	33.7	34.5	30.2	27.5	5.23	4.93	4.04	2.35	**0.0053**	0.0044	0.0031	0.0016
***	6	0.0079	38.1	42.5	37.5	34.4	5.91	5.62	4.61	2.71	0.0048	0.0039	0.0027	0.0014
	7	**0.0053**	**42.1**	**52.1**	**46.4**	**42.9**	**6.71**	**6.48**	**5.38**	**3.30**	0.0042	0.0034	0.0024	0.0012
	8	0.00351	45.2	63.6	57.5	53.5	7.83	7.97			0.0037	0.0030	0.0021	0.0011
	9	0.00234	48.7	71.8	71.5	66.6					0.0032	0.0026	0.0018	0.0009
***	1	0.060	9.4	11.9	7.3	6.5	0.88	0.83	0.83	0.60	0.0019	0.0012	0.0016	0.0012
	2	0.040	13.3	15.1	9.4	8.4	1.14	1.09	1.01	0.72	0.0018	0.0012	0.0015	0.0011
	3	0.027	18.6	19.1	12.1	10.7	1.49	1.43	1.23	0.86	0.0017	0.0012	0.0014	0.0010
San	4	0.0178	23.8	24.0	15.6	13.8	2.00	1.90	1.49	1.02	0.0015	0.0012	0.0014	0.0009
Fernando	**5**	**0.0119**	**30.4**	**30.1**	**20.5**	**17.7**	**2.86**	**2.64**	**1.88**	**1.22**	0.0013	0.0012	0.0013	0.0008
	6	0.0079	38.8	37.8	27.3	22.7			2.51	1.48	0.0012	0.0012	0.0012	0.0008
	7	0.0053	49.2	47.4	35.2	29.2				2.03	0.0012	0.0011	0.0011	0.0007
	8	0.00351	61.9	59.4	44.1	38.6					0.0012	0.0011	0.0010	0.0006
	9	0.00234	76.7	74.4	56.3	51.1					0.0011	0.0010	0.0009	0.0005

* structure's inherent damping 2.5% *** sufficient control strength for acceptable drift ratio ** drift/3m **<**1/200 acceptable; >**1/200 unacceptable**

The drift ratio, calculated as the story drift per unit height, was limited to an arbitrary value of 1/200 as a design target. It is noted that as the control becomes stronger (by choosing a small value of R_{factor}), a point is reached where the displacements become so small that the brace, due to its flexibility, is no longer capable of supporting a slip load through a deformation sufficient to dissipate the required energy. At the threshold where this limit is reached, the performance of the friction damper is essentially at its optimum. Therefore, it is postulated that the friction damping distribution and structural performance obtained at this level correspond to the optimal friction dampers that would be determined by trial and error.

Figures 5 (a) and (b) illustrate how these optimal slip loads compare to the optimal slip loads obtained in [1] using a Level Set Programming (LSP) technique, a trial and error technique that uses random sampling and consecutive narrowing of the 4-dimensional search space to arrive at a final set of slip loads. The LSP technique was applied using performance indices constituted by total energy and by maximum drift with the objective being to minimize the total energy and to minimize the maximum drift respectively.

It is first noted that the LSP obtained slip loads for the max drift performance function are significantly higher than that obtained using the total energy. While the absolute value of the slip loads at the base are well predicted for the El Centro record input, the distribution of the slip loads obtained does not match the trend obtained by LSP. With the San Fernando record, the opposite is observed; the trend in the slip loads appears similar to that obtained using LSP, but the absolute value of the slip load obtained at the base was found to exceed that determined using LSP by a significant margin. It should be noted that the fit with the

LSP determined slip loads is not expected to be precise due to the fact that the response of the structure is relatively insensitive to the magnitude of the slip load near optimal. Therefore, the lack of a precise fit does not indicate a poor performance, but does indicate that further work is necessary to understand the differences between the LSP results and the proposed modal analysis technique.

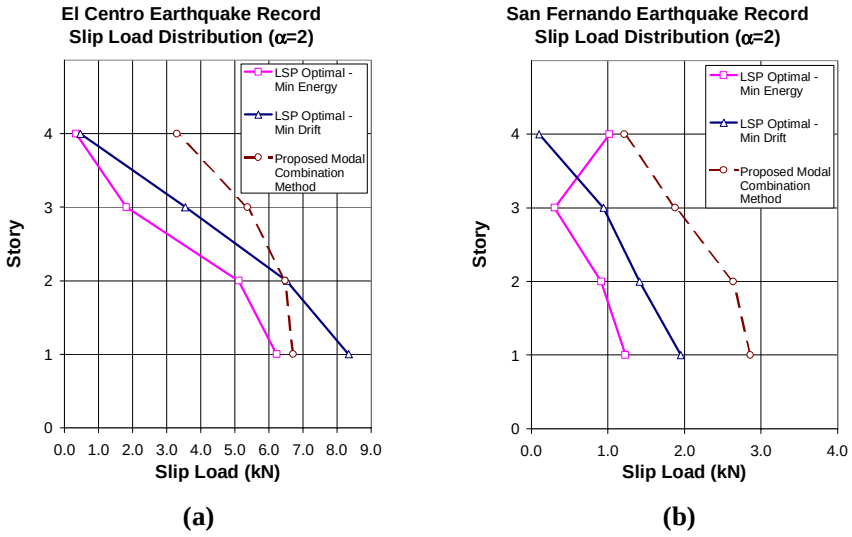

Figure 5. Comparison of proposed modal combination method slip load prediction with results obtained using level set programming with (a) El Centro and (b) San Fernando earthquake record input.

6-STORY ECCENTRIC BUILDING

A 3-D frame was modeled after an existing RC structure studied by H.K. Dengenkolb Associates [7] following the California 1989 Loma Prieta earthquake. Figure 6 contains a description of the geometry of the model and an indication of how the 18DOF model was extracted. Discretization of the model as shown in Figure 6 presumes that the floors behave as rigid diaphragms. The mass and stiffness coefficients for each story are summarized in Table 3. The eccentricity of the first floor mass and stiffness introduces a coupling of the transverse and torsional vibration modes. While the original structure was found to have a dominant soil-structure interaction, this would interfere with the ability to study the control technique, therefore the model generated for analysis did not include foundation compliance. The lateral and rotational stiffness properties were selected so as to match the frequencies of the first longitudinal and the first coupled lateral-torsional modes of the model to that observed in the original structure. Consequently, the model adapted for this study control is much less stiff than the original structure. Table 4 gives the modal frequencies and mode shape descriptions for the model structure.

Raleigh damping was used to account for damping inherent in the structure. Damping was assumed to be approximately 2% in first two modes, and set proportional to the mass and stiffness matrices using proportionality factors α=0.34 and β=0.001. The El Centro record described above was used for the analysis, with the N00E component acting in the transverse (X) direction and the S90W component acting in the longitudinal (Y) direction. No vertical excitation was incorporated into the analysis. The Q matrix was chosen such that the first term of the performance index (Equation 5) to correspond to the sum of

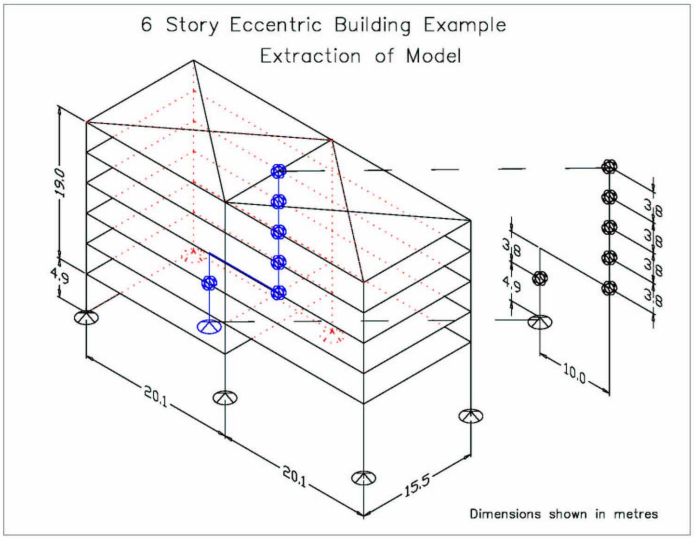

Figure 6. 6-story eccentric building frame – extraction of model.

Table 3. Story Mass and stiffness Parameters: (SI Units)

Story	Height (m)	Mass		Stiffness		
		Translation (tonne)	Rotational (tonne-m^2)	Transverse (kN/mm)	Longitudinal (kN/mm)	Torsional (kN-m/rad)
1	4.88	526	14020	2562	2907	2.845E+08
2	3.81	716	85164	3440	3723	3.642E+08
3	3.81	716	71860	3440	3723	3.642E+08
4	3.81	716	71860	3440	3723	3.642E+08
5	3.81	716	71860	3440	3723	3.642E+08
6	3.81	585	71065	3440	3723	3.642E+08

Table 4. Selected mode shapes and frequencies.

Mode No.	Frequency (Hz)	Mode Description*	Mode No.	Frequency (Hz)	Mode Description*
1	1.79	XT-1	…	…	…
2	2.74	L-1	14	20.71	XT-10
3	2.97	XT-2	15	21.04	L-5
4	6.99	XT-3	16	22.60	XT-11
5	8.19	XT-4	17	22.64	L-6
6	8.26	L-2	18	30.74	XT-12

*-"XT-n" indicates the nth transverse-torsional mode and "L-n" represents the nth longitudinal mode.

potential and kinetic energy, while the R matrix was set to the identity matrix multiplied by a factor (R_{factor}). The single variable, R_{factor}, was used to provide a means of adjusting the level of control.

Two damper configurations are reported herein. Configuration 1 comprises 23 dampers in total: one in one bay in each of all four sides from the base to the top. Configuration 2 comprises 17 dampers in total: one in each bay of each end acting in the transverse direction (11) and one in one bay per story on one side only of the structure acting in the longitudinal direction (6).

Configuration 1 was chosen as a likely first-choice damping scenario. Although this configuration is expected to be highly effective, it requires a large number of dampers. Except for the first story there are 4 dampers per story, but only 3 degrees of freedom, therefore one of the dampers is redundant in each of the stories. In retrofit construction, the costs associated with installing a damper, including relocation of tenants, removal and reconstruction of architectural finishes may outweigh the costs of the structural modifications, therefore it is understandable that using this large number of dampers is not necessarily the most cost effective choice.

Configuration 2 represents a more cost effective damper arrangement, utilising a reduced number of dampers distributed along the height. This unsymmetrical distribution is one that may not be considered by a designer. However, it would provide significant cost savings and has been shown to provide a similar performance level to Configuration 1.

Configuration 1 Results

Figure 7 shows the distribution of the viscous dampers for Configuration 1 based on using R_{factor}=5x10e-4. The damping coefficient is indicated both numerically and graphically through the line weight of the damper and the diameter of the circle. The peak displacements in the longitudinal direction were found to be about 13mm in the longitudinal direction and 10mm in the lateral direction. In general it was observed that the larger dampers were found near the base and in the large open bay at the end of the building with damping coefficients becoming progressively smaller towards the top stories.

The friction damper slip loads corresponding to the already determined viscous dampers in each of the proposed dampers were evaluated by matching the energy dissipated at the peak cycle. It was assumed that the brace stiffness is high such that he slip loads converge to $(\pi/4)u_{max}$. The resulting damper distribution is shown in Figure 8 with slip loads (in kips) indicated numerically. Due to the larger damper displacements and velocities experienced in the lower stories and particularly the two story end bay, the slip loads distribution is more pronounced than that of the viscous dampers with a steeper decline in the values of slip load from the base up than with the viscous damping values.

Configuration 2 Results

Viscous dampers damping coefficients designed using the RSA procedure are shown in Figure 9 together with the numerical values of the damping coefficients. The maximum longitudinal displacement at the top in this case was 13mm, identical to that of configuration 1, however, the lateral deflection at the top was larger at 12mm. The damping coefficients in the end frames, acting in the transverse direction were found to be nearly identical. In the longitudinal direction, however, the single damper damping coefficient is less than the combined total of the two damping coefficients in Configuration 1. This indicates that the total required damping capacity in configuration 2 is not as great.

The slip force computed for each friction damper is illustrated in Figure 10. The reduction in slip load capacity in the longitudinal direction is significant. Whereas Configuration 1 requires a total slip load capacity of 3600kN in two friction dampers in the longitudinal direction on the first story, the total capacity in Configuration 2 at the same story level is reduced to 2740kN in a single damper. Consequently, the case is made that the non-symmetrical damper configuration of Configuration 2 provides an advantage over Configuration 1 not only in terms of a less invasive retrofit, but also a potential reduction in the total capacity of dampers.

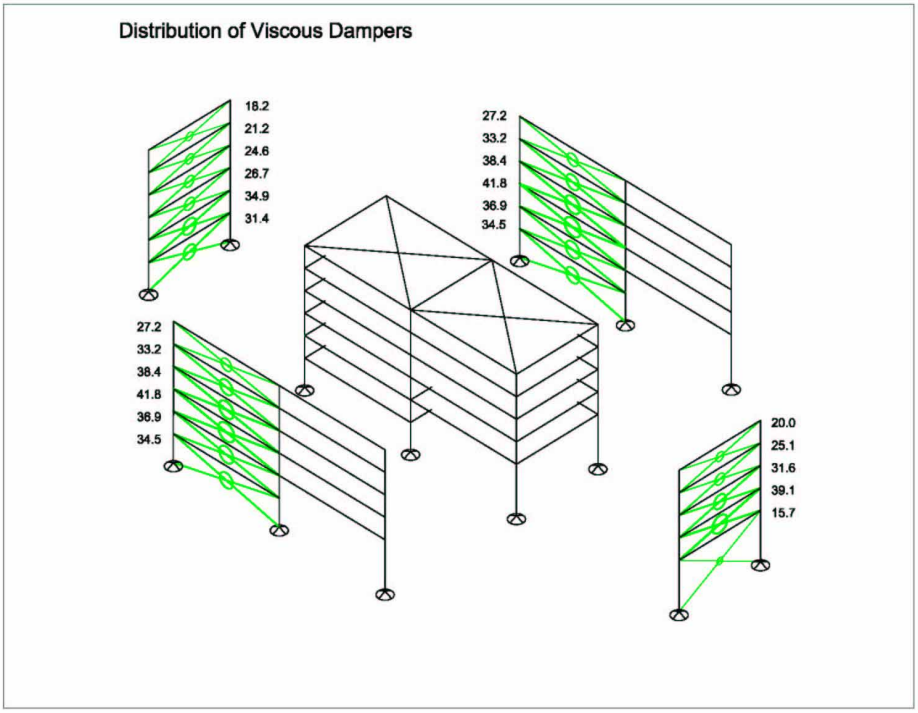

Figure 7. Configuration 1 viscous damper damping coefficients. (in kN-s/mm)

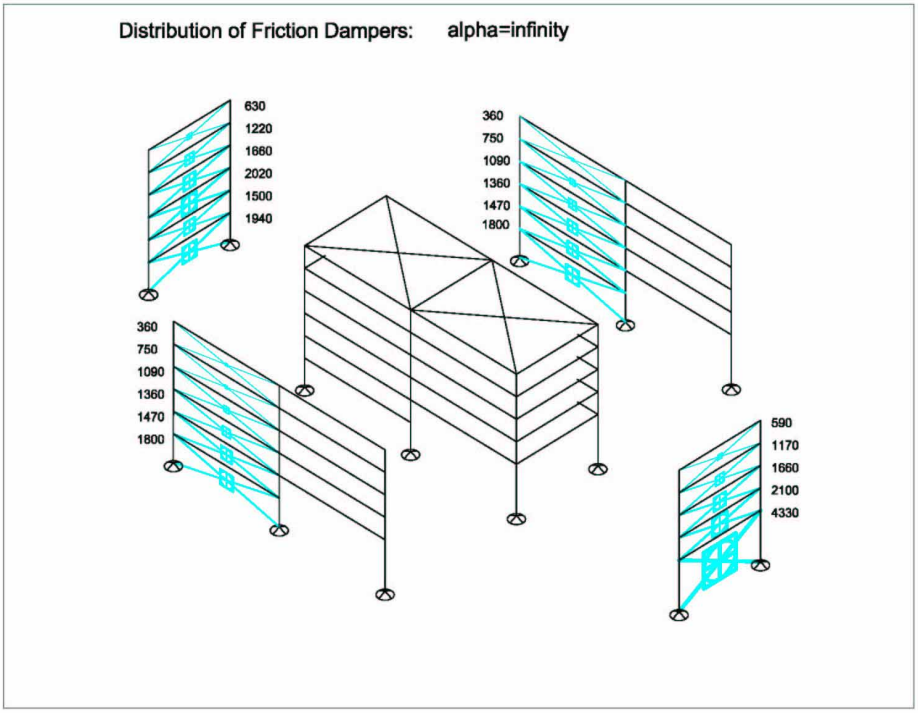

Figure 8. Configuration 1 friction damper slip loads. (in kN)

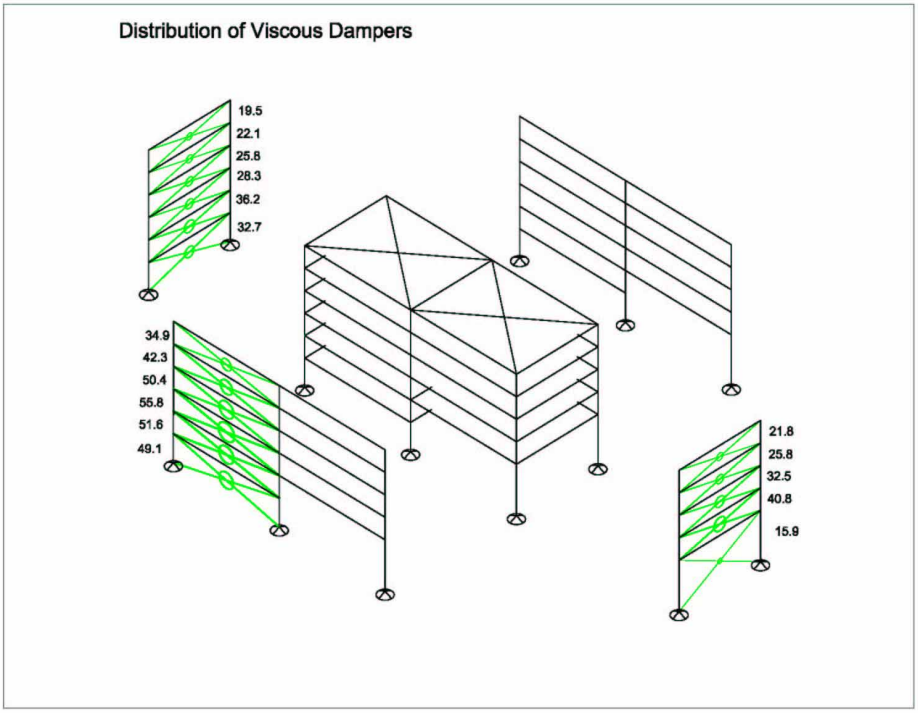

Figure 9. Configuration 2 viscous damper damping coefficients. (in kN-s/mm)

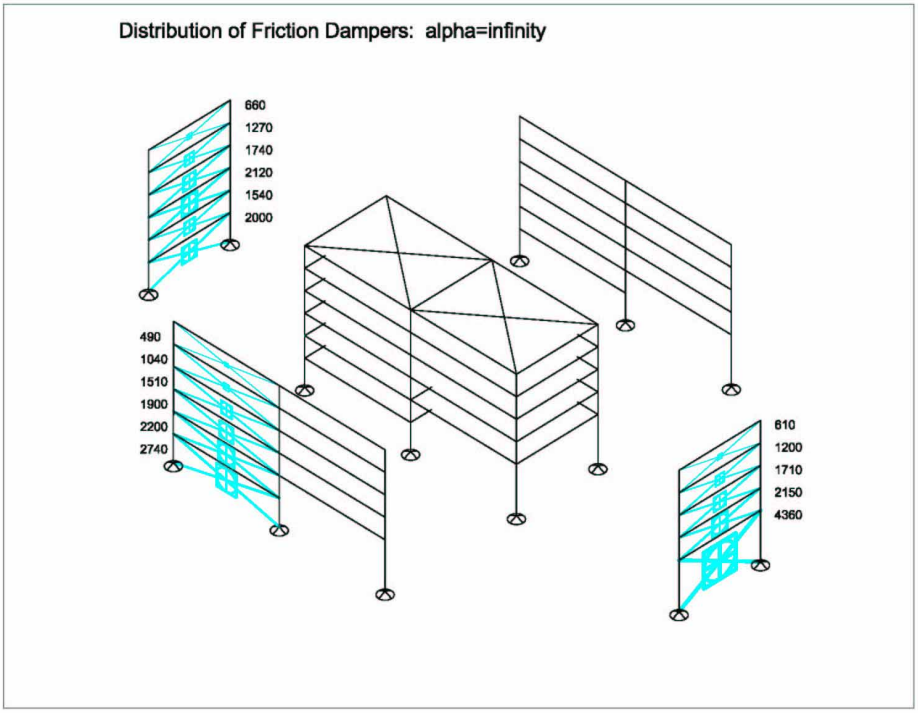

Figure 10. Configuration 2 friction damper slip loads. (in kN)

CONCLUSIONS AND RECOMMENDATIONS

Conclusions

A method of using structural control concepts to size passive viscous and friction dampeer at pre-delected locations in structures has been proposed. It has been demonstrated that using peak cycle forces and observed velocities, passive control nearly equivalent in strength to the fully active system could be obtained. Using the concept of equal peak cycle energy dissipation and recognising that braces supporting friction dampers have some undesirable flexibility, friction slip loads could be determined. Utilising this concept led to a definition of the optimal friction damper acting at its limit to produce minimum deflections. As was shown, the level of damping incorporated does not necessarily have to satisfy this limit, and lesser slip loads may be sufficient to satisfy performance criteria, in this case given as an arbitrary upper limit on the drift ratio.

Using a more complex example of an 18DOF eccentric structure with coupled lateral and torsional modes, the proposed design procedure was demonstrated to be capable of producing reasonable estimates of viscous damper damping coefficients and friction damper slip loads. Two sets of selected damper loacations were compared leading to the conclusion that the proposed method is useful in helping to explore various retrofit concepts.

Recommendations

It is recommended to further explore the proposed methodology. Response Spectral Analysis procedures such as the Complete Quadratic Combination (CQC) are often used in practice to account for closely spaced modes. However, there is no equivalent procedure developed for the case of combining complex modes of non-classically damped structures. Further work in this area would be helpful to improve the accuracy of computed response quantities.

RSA procedures as formulated herein require the computation of two surfaces that together relate structural response its damping and frequency. It is recommended to further explore the development of design spectra based on these these functions to facilitate design of structures with high damping and non-classical damping.

REFERENCES

1. Dowdell, D.J. and Cherry, S. “On Passive and Semi-Active Friction Dampers for Seismic Response Control of Structures,” Eleventh World Conference on Earthquake Engineering, June 22-28, Acapulco, Mexico, 1996
2. Reinhorn, A.M., Gluk, N., Gluk, J., and Levy, R. “Optimal Design of Supplemental Dampers for Control of Structures,” 11th European Conference on Earthquake Engineering. AA Balkema Rotterdam Reinhorn Gluk Gluk and Levy 1998
3. Dowdell, D.J., 2003, Friction and Hysteretic Dampers for the Seismic Response Control of Structures, PhD Thesis in draft, University of British Columbia
4. Dowdell D.J. and Ventura, C.E. “Determining optimal damper sizes in a steel frame structure using structural control concepts” in STESSA 2003 Behaviour of Steel Structures in Seismic Areas Ed. F. M. Mazzolani, Swets and Zeitlinger, 2003
5. Meiroivtch, L., *Dynamics and Control of Structures*, John Wiley & Sons, 1990
6. Soong, T.T., *Active Structural Control Theory and Practice*, Longman Scientific & Technical, 1990.
7. H.K. Dengenkolb Associates, “Effects of the Loma Prieta Earthquake on the Veterans Administration Palo Alto Medical Center”, October 4, 1991.